Petroleum and Coal

Article **Open Access**

Estimates of Geothermal Gradient of Part of the Mid-Niger Basin, Nigeria From Spectral Inversion of High-Resolution Aeromagnetic Data: Implications for Hydrocarbon and Geothermal Energy Prospectivity

A. I. Opara[1], V. U. Nwofor[1], A. C. Ekwe[2], C. N. Okereke[1], H. N. Echetama[1], and J. O. Ibezim[3]*

[1] *Department of Geology, Federal University of Technology, Owerri, Nigeria*
[2] *Department of Geology/ Geophysics, Federal University Ndufu-Alike Ikwo, Abakaliki, Nigeria*
[3] *Department of Physics, Imo State University Owerri, Nigeria*

Received February 27, 2020; Accepted June 3 2020

Abstract

Curie point depth, geothermal gradient, and heat flow values of part of the Mid-Niger Basin, Nigeria were estimated using high-resolution aeromagnetic data of the study area. Spectral inversion of high-resolution aeromagnetic data was used to estimate the top and centroid depths of the magnetic sources which were further applied to calculate the Curie point depths of the magnetic sources. Top depths to the magnetic sources across the area are of the range of 1.865 km to 4.264 km with a mean of 2.723 km whereas the centroid depths of the magnetic sources are of the range of 13.26 km - 17.12 km with a mean value of 14.78 km. The range of values for the Curie point depth values are from 24.21 km to 32.26 km with an average value of 26.83 km. The geothermal gradient values were estimated to be of the range of 17.98 - 23.95^{o}C/km with an average value of 21.62^{o}C/km. Finally, the heat flow values range from 44.95 mWm^{-2} to 59.89 mWm^{-2} with an average value of 54.04mWm^{-2}. It was observed that the range of estimated geothermal conditions in the study area point to the fact that the area is not a volcanic or thermally active region and therefore has no potential geothermal energy reservoirs. Finally, the estimated geothermal gradient in this study may not be enough to cause thermal maturation of the available source rocks in the area.

Keywords: *Aeromagnetic; Curie point depths; Geothermal gradient; Heat flow; Spectral inversion; Hydrocarbon prospectivity.*

1. Introduction

The Mid-Niger basin has not been fully studied and explored like other inland basins and its petroleum potentials are not yet fully known. This is because the potential non-marine source rocks of the southern Mid-Niger basin are believed to have not been deeply buried especially within the margins and therefore are believed to be thermally immature [1-3]. In addition, because of the power challenges of Nigeria and the discovery of several hot springs across Nigeria, a lot of interests have been generated towards the possibility of the development of geothermal reservoirs. Therefore, exploration activities for the discovery of geothermal reservoirs across the country especially using high resolution aeromagnetic data have been intensified [4-5]. Therefore, heat flow and hydrocarbon potential studies in the Mid-Niger Basin are still poorly understood, due in part to the dearth and distribution of subsurface data. This studies is very important because there is a well-established and defined relationship between geothermal gradient, sedimentation, vitrinite reflectance, thermal maturation of organic materials, and type of hydrocarbon generated [1,3,6-7]. Moreover, because of the intense tectonic activities associated with the study area and the high density of faults in the study area, it might not be easy to monitor thermal conductivity patterns and heat flow systems associated with the lower crustal heat flow. Although heat flow observations can be made from boreholes on land and data measured in the deep-sea sediments, the obtained values generally are insufficient in determining regional thermal structures [8].

Curie point depth based on spectral inversion of magnetic data has widely been used in the estimation of regional thermal structures worldwide [9-10]. At curie temperatures, a magnetic a substance loses its magnetic polarization. Consequently, it may be possible to locate a point on the isothermal surface by determining the depth to the bottom of a polarized rock mass [11]. Curie point depth is the depth at which the rock loses their ferromagnetic properties due to increase in the temperature above the curie temperature which is approximately 580°C; in other words, it is a depth at which a magnetic material passes from a ferromagnetic state to a paramagnetic state under the infuence of increasing temperatures [4,12]. Though the concept of Curie point temperature may be controversial, Curie point depth (CPD) has been described by many authors [5,9,12-15]. CPD has been applied over the years in the estimation of thermal structure in various regions, and is often classified into two categories. They include the determination and examination of the shape of isolated magnetic anomalies [9,16] analysis of the statistical properties of the patterns of the magnetic anomalies [10]. The first method provides the relationship between the spectral characteristics of the magnetic anomalies and the depth of the magnetic sources by carrying out Fourier synthesis of the spatial data. The latter method is believed to be more appropriate in the compilation of magnetic anomalies [12,17].

Spectral inversion techniques have been very effective in inferring the depths to magnetic sources because its operations are done in the frequency domain [10]. The technique has revealed that when a statistical population of a potential field source exists at around a specific source depth, then the expression of those sources on a plot of the natural logarithm of energy against wavenumber is a straight line having a slope of - $4\pi h$ [10]. In heat flow estimation from aeromagnetic data, spectral inversion is usually carried out on the residual data to infer the top depths of magnetic sources (Z_t), and the centroid depths of the magnetic source (Z_o) for the estimation of Curie point depths (CPDs). Several approaches have been used by several authors to acquire the depths to magnetic anomalous sources and centroid depths using the spectral inversion of high-resolution aeromagnetic (HRAM) data [4,18-22]. The CPD is symbolically represented as Z_b; the depth to the bottom of magnetic sources (DBMS). It is described as such because at such depth, the dominant magnetic minerals in the crust passes from the ferromagnetic state to a paramagnetic state under the influence of increasing temperatures [23].

The centroid depths are the geometric centres [15] of the vertical rectangular prismatic bodies [10]. Bhattacharyya [24] used an expression for the power spectrum of the total magnetic field intensity over a single rectangular block, which was generalized by Spector and Grant [10] by assuming that the anomalies on an aeromagnetic map are due to an ensemble of vertical prisms. Bhattacharyya and Len [9] and Okubo *et al*. [15] also described Z_b as the basal depth of the magnetic sources which is assumed to be the CPD of the area hosting the magnetic sources. Several methods exists for the estimation of Curie point depth [25-27]. Spector and Grant [10] examined the pattern of the anomalies and provided the relationship between the spectrum of the magnetic anomalies and the depth of a magnetic source by carrying out a Fourier transform of the spatial data into the frequency domain. Okubo *et al.* [25] summarized the methods of estimating the depth extent of magnetic sources. According to Okubo *et al.* [25], the methods can be categorized into two groups: the group that examines the shapes of isolated magnetic anomalies [9] and the group that examines statistical properties of patterns of magnetic anomalies [10]. Both groups provide the relationship between the spectrum of magnetic anomalies and the depth of magnetic source by transforming the spatial data into the frequency domain.

The aeromagnetic data used in this study is composed of four (4) high resolution aeromagnetic maps of the Nigeria Geological Survey Agency (NGSA) which include Gulu, Koton-Karfi, Abaji, and Kuje. The main objective of this study is to evaluate the geothermal conditions of the study area through the estimation of the Curie point depths, geothermal gradients, and heat flow. These will be used to evaluate the geothermal potentials of the area as well as infer the possible influence of the geothermal gradient on hydrocarbon generation.

1.1. Geology of the study area

The study area is located between latitudes $8^{0}00^{1}$ N - $9^{0}00^{1}$ N and longitudes $6^{0}30^{1}$ E - $7^{0}30^{1}$ E and constitutes part of the southern Mid-Niger Basin. The Mid-Niger Basin is a NW-SE trending intra-cratonic sedimentary basin extending from Kontagora within the basement complex of Northern Nigeria to Lokoja and environs within the Cretaceous sediments of the south. The Bida basin, also known as the Mid-Niger or Nupe basin located in north-central Nigeria is one of the Cretaceous basins in West Africa whose origin is associated with the opening of the South Atlantic. The Southern Mid-Niger basin has an average sedimentary thickness of 3.5 km thick [1,3]. The study area is surrounded by Precambrian basement rocks which experienced intense tectonism during the Late Pan-african phase (600±150 m.y). These Pan-African episodes resulted to the development of shear zones that were subsequently reactivated during the Late Campanian-Maestrichtian resulting in wrench faulting which later formed the basin [1-3]. Ladipo [28] suggested that the Mid-Niger Basin is a gently down-warped trough whose origin is closely connected with the Santonian orogenic movement in south eastern Nigeria and the Benue valley, with its sedimentary fill comprising of post-orogenic molasses and thin, unfolded marine sediments. The basin trends in the NW-SE direction, a NW extension of the Anambra Basin perpendicular to the main axis of the Benue Trough as shown in Figure 1.

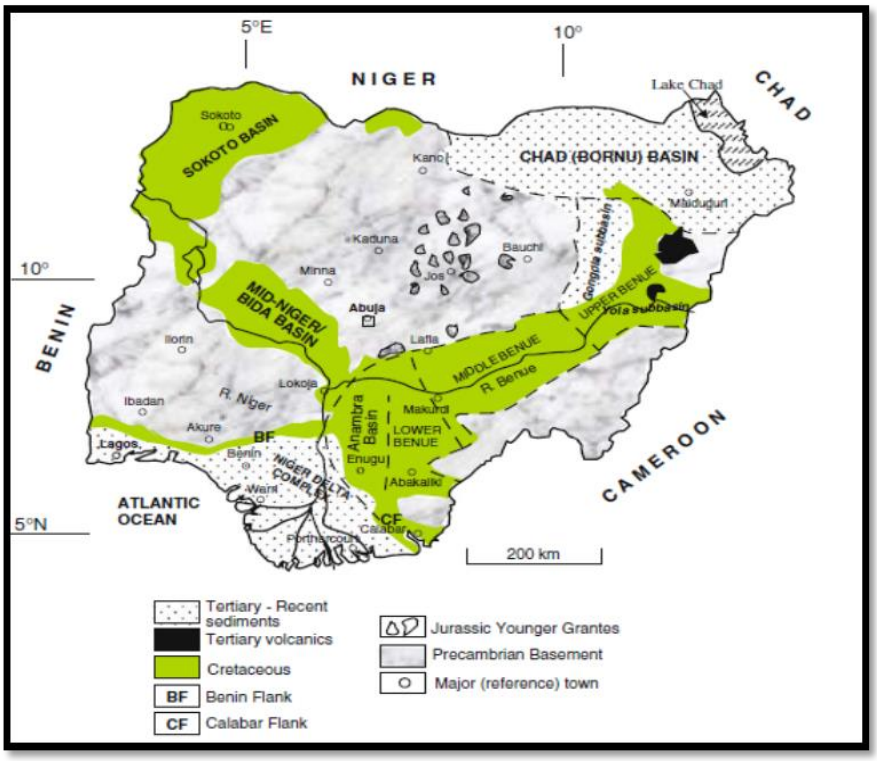

Figure1. Geological map of Nigeria showing the Mid-Niger Basin [29]

The Mid-Niger Basin and the Anambra Basin were the major depocentres during the third transgressive cycle in the late Cretaceous. Notable geologists that have worked in the area have divided this basin geographically into the northern and southern Bida Basin, probably due to the rapid facies changes across the basin [2-3,29-30]. The northern and southern Bida Basins comprise of about 3 km thick Campanian to Maastrichtian continental to shallow marine sediments [2,30, 30-31]. The southern Bida Basin comprises the basal Campanian Lokoja Formation, followed by the Maastrichtian Patti Formation and then the youngest Agbaja Formation which is also Maastrichtian in age [2,28,31]. Their lateral stratigraphic equivalents in the northern Bida Basin consist of the basal Bida Formation as shown in Figures 2&3.

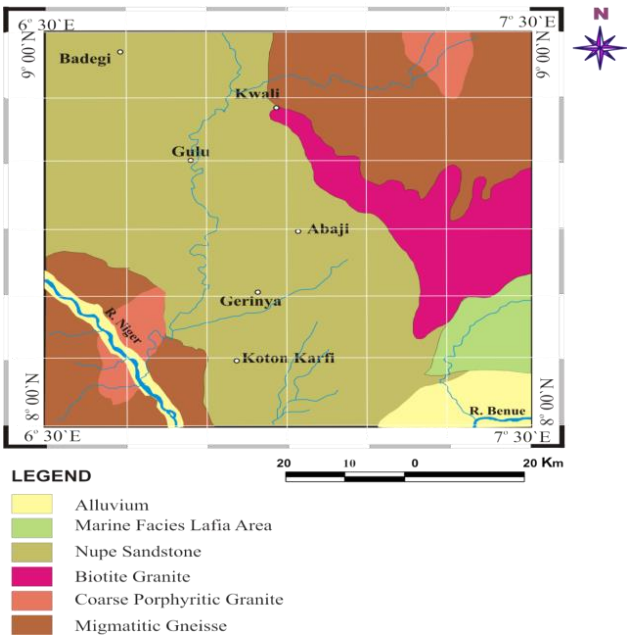

Figure 2. Geological map of part of the southern Mid-Niger Basin

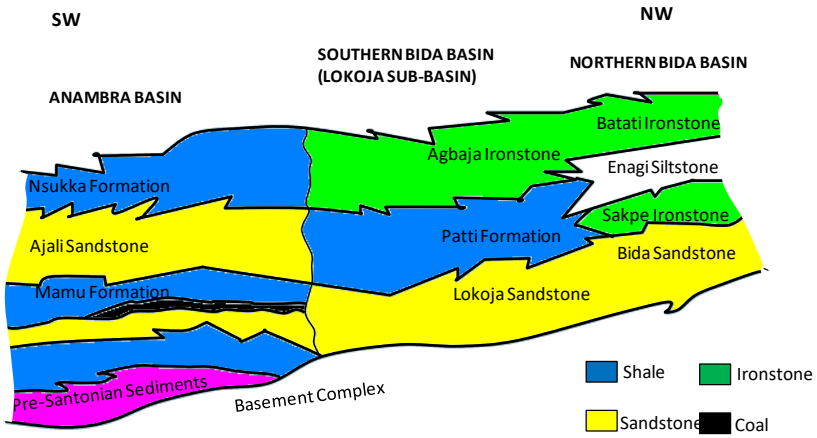

Figure 3. Lateral stratigraphic equivalents of the northern Bida Basin, southern Bida Basin and Anambra Basin [2].

Gravity studies over the Bida Basin estimated that the sediments which include the Bida , Enagi and Batati Formation (ironstone) makes up a maximum sedimentary thickness of about 3.5 km in the central axis [32]. However, a recent spectral analysis of the residual total magnetic field in different sections of the basin revealed an average sedimentary fill of about 3.4 km with basement depth of up to 4.7 km estimated in the southern and central parts of the basin [35]. In general, the depth to the basement in the basin is believed to decrease smoothly from the central parts to the flanks of the basin [1-3,28,30].

2. Materials and methods

2.1. Data

Digitized high revolution aeromagnetic (HRAM) maps of sheets 206, 207, 227, and 228 at a scale of 1:100,000 covering a total area of about 12,000km^2 was used in this study. The study area as shown in Figure 2 has important towns like Gulu, Koton-Karfi, Abaji, and Kuje. The high resolution aeromagnetic data was acquired for the Nigerian Geological Survey Agency by Fugro between 2006 and 2009. The aeromagnetic survey was flown along a series of NW-

SE flight lines with 500m line spacing, 80m terrain clearance and flight line direction of NW-SE. Data were recorded at very small intervals of 0.1s each with 80 m normal flight height. The geomagnetic gradient was removed from the data using January 2005 IGRF model referenced to the World Geodetic System, 1984 ellipsoid. The aeromagnetic survey was flown along with a series of NW-SE flight lines (perpendicular to dominant regional geologic strike) spaced at 500 m with 2000 m tie line spacing in the NE – SW direction.

2.2. Methods

The regional - residual separation technique using polynomial fitting was carried out in this study. This is a purely analytical method in which matching of the regional field by a polynomial surface of low order exposes the residual features as random errors. The regional gradients were removed by fitting a plane surface to the data by using multi- regression least-squares analysis to obtain the residual data. Figures 4 and 5 show the total magnetic field intensity (TMI) and residual field maps of the study area respectively. These maps revealed magnetic highs at the margins while magnetic lows with magnetic intensity values between -920-149 gammas are concentrated at the central parts of the maps.

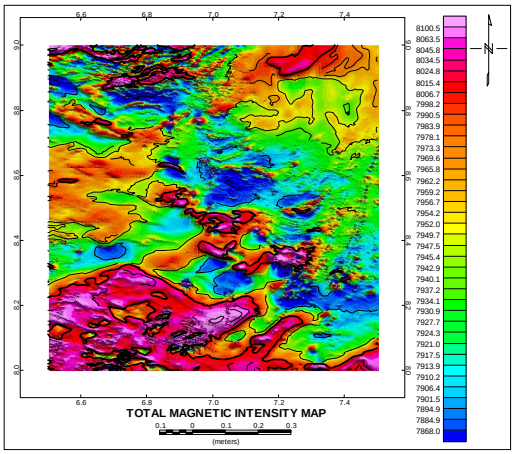

Figure 4. First Degree Total Magnetic Field Intensity of the Aeromagnetic data of the study area in gamma

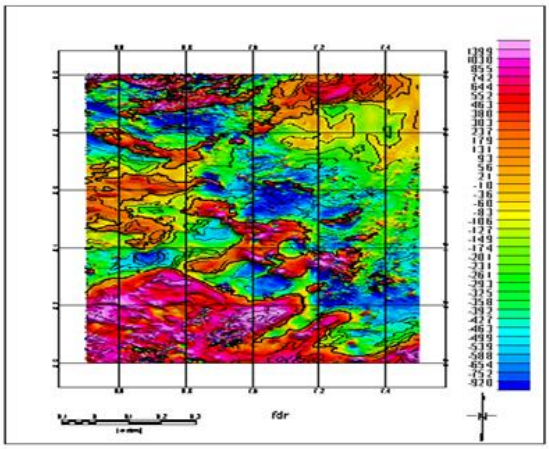

Figure 5. First Degree Residual Map of the Aeromagnetic Data in gamma

2.3. Curie Point depth estimation

Curie point depth (CDP) estimation based on spectral inversion of magnetic data has been widely used in the estimation of regional thermal regimes worldwide [10-11,27]. The technique is generally similar to that used in earlier studies by Spector & Grant [10]. The depth to the top of the magnetic body (top bound) (Z_t) and the centroid of the magnetic source (Z_o) were calculated using the power spectrum of the magnetic anomalies, which was further used in the calculation of the depth to the magnetic source (Curie point depth). In using the method presented by Tanaka *et al.* [27], it was assumed that the layer extends in infinitely far distances in all horizontal directions. The depth to the top of the magnetic source is therefore seen to be very small when compared with the horizontal scale of the magnetic source, and the magnetization M(x, y) is a random function of x and y. Blakely [34] introduced the power spectra of the total field anomaly $\Phi_{\Delta T}$ given as:

$$\Phi_{\Delta T}\left(k_x, k_y\right) = \Phi_{\mathrm{M}}\left(k_x, k_y\right) \times \quad F\left(k_x, k_y\right), \qquad (1)$$

$$F\left(k_x, k_y\right) = 4\pi^2 C_m^2 |\Theta_m|^2 \left|\Theta_f\right|^2 e^{-2|k|Z_t}, \qquad (2)$$

Where; Φ_{M} = the power-density spectra of the magnetization; C_m = proportionality constant; and, Θ_m and Θ_f = factors of magnetization direction and geomagnetic direction, respectively.

Equations 1&2 can then further be simplified by noting that all terms except $|\Theta_m|^2\left|\Theta_f\right|^2$ are radially symmetrical, though the radial averages $|\Theta_m|^2\left|\Theta_f\right|^2$ are constant. If M(x, y) is completely

random and uncorrelated, $\Phi_M(k_x, k_y)$ is therefore a constant. Hence, the radial average of $\Phi_{\Delta T}$ is given as:

$$\Phi_{\Delta T}(|k|) = Ae^{-2|k|Z_t}\left(1 - e^{-|k|(Z_b - Z_t)}\right)^2, \quad (3)$$

where A = constant; and k = wave number

For wavelengths less than about twice the thickness of the layer, Equation (3) approximately becomes

$$\ln\left[\Phi_{\Delta T}(|k|)^{1/2}\right] = \ln B - |k|Z_t, \quad (4)$$

where B is a constant.

The upper bound of the magnetic source Z_t can be estimated by fitting a straight line to the high-wave number part of a radially averaged power spectrum given as $\ln\left[\Phi_{\Delta T}(|k|)^{1/2}\right]$. Based on the foregoing therefore, and by combining equation 3&4, equation 5 is derived:

$$\Phi_{\Delta T}(|k|)^{1/2} = Ce^{-|k|Z_o}\left(e^{-|k|(Z_t - Z_o)} - e^{-|k|(Z_b - Z_o)}\right), \quad (5)$$

Where C is a constant. At longer wavelengths, equation 5 becomes:

$$\Phi_{\Delta T}(|k|)^{1/2} = Ce^{-|k|Z_o}\left(e^{-|k|(-d)} - e^{-|k|(d)}\right) \approx Ce^{-|k|Z_o}2|k|d, \quad (6)$$

Where 2d is the thickness of the magnetic source. Solving completely from equation 6, equation 7 shown below is derived:

$$\ln\left\{\left[\Phi_{\Delta T}(|k|)^{1/2}\right] / |k|\right\} = \ln D - |k|Z_o \quad (7)$$

The top bound and the centroid of the magnetic source can be estimated by fitting a straight line through the high wave number and low wave number parts of the radially averaged spectrum of $\ln\left[\Phi_{\Delta T}(|k|)^{1/2}\right]$ $\ln\left\{\left[\Phi_{\Delta T}(|k|)^{1/2}\right] / |k|\right\}$. The top-bound and centroid depth of the magnetic source is therefore estimated from the slope of the power spectrum as carried out by earlier scholars [15,27,35-38].

To compute the depth to to the Curie Point Depth, the residual magnetic field data of the study area was divided into overlapping grids with spectral widths of 135 x135 km. The dimensions of the square grids used were based on a minimum ratio of 12:1 of block size to prism dimensions (magnetic sources) as demonstrated by Tselentis [39]. Thus assuming a minimum anomaly of approximately 4km, this meant a minimum block size of about 55km. Upward continuation technique was utilized for each block to get rid of the short-wavelength components of the magnetic data with the continuations made at the elevations of 1 to 4km. The obtained basal depth (Z_b) of magnetic sources is assumed to be the Curie point depth [9].

In this study, the method adopted is similar to the method of Okubo et al. [15]. The top boundary and the centroid of a magnetic source Z_t and Z_o respectively were calculated from the power spectrum of magnetic anomalies, and were used to estimate the basal depth of the magnetic sources, Z_b, through the equation 1 [15,40]. The depth to the magnetic sources (Curie point depth) is thus derived using equation 8:

$$Z_b = 2Z_o - Z_t \quad (8)$$

where Z_o= Depth of the centroid of magnetic source, Z_t= Top Bound and Z_b= Curie point depth.

2.4. Geothermal gradient and heat flow estimation

Due to the absence of heat flow data in the study area, a dimensional heat conductive transport model was used to estimate the heat flow and geothermal gradient. This model is based on Fourier equation. In a one dimensional case, making the assumption that the direction of temperature is vertical and the temperature gradient dT/dZ constant, the Fourier law takes the form of equation 9:

$$q = \lambda \frac{dT}{dZ} \quad (9)$$

Where q = heat Flow and λ = coefficient of thermal conductivity. According to Tanaka *et al.*, [27], the Curie temperature (θ_c) is defined as

$$\theta = \left[\frac{dT}{dZ}\right]Z \quad (10)$$

Applying equations (9) and (10) in establishing the relationship between Curie point depth (Z_b) and heat flow (q), q was therefore estimated using equation 11:

$$q = \lambda\left[\theta/Z_b\right] = \lambda(580°C/Z_b) \quad (11)$$

Equation 11 shows that the CPD is inversely proportional to the heat flow, q. Similarly, the geothermal gradient was estimated from equation 10. In both estimations, the Curie point temperature of 580°C and thermal conductivity of 2.5 $Wm^{-1o}C^{-1}$ was assumed [36,43].

3. Results and discussion

The sample graphs of the logarithms of the energy spectrum for some of the spectral blocks using the FOUR POT™ software are shown in Figure 6. Figure 7 shows the spectral blocks showing the estimated CPD, geothermal gradients and heat flow of the study area while the summary of the estimated CPD, geothermal gradients and heat flow of the study area are shown in Table 1. Similarly, Figure 8 shows the spatial map of the Curie Point Depths while Figure 9 is the spatial map of the geothermal gradient estimated from the study area. Figures 10,11 &12 are the spatial map of the heat flow, the cross plot of Curie point Depth versus Geothermal gradient and the Cross plot of Curie point Depth versus Heat Flow respectively.

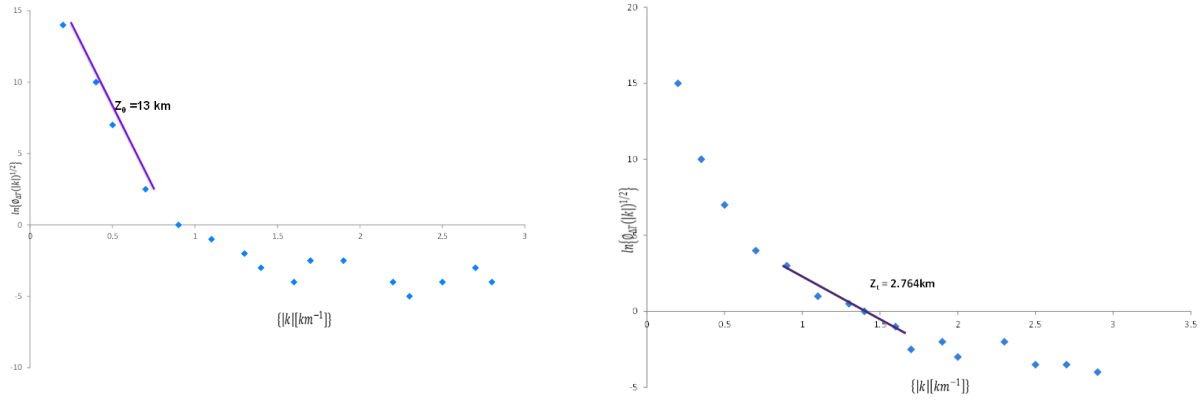

Figure 6. Plots of the logarithms of the spectral energies for some of the spectral blocks: (a) Z_0 and (b) Z_t

Table 1. Estimated CPD, geothermal gradients and heat flow of the study area

Spectral blocks	Longi-tude		Lati-tude		Depth	(km)	CPD(km)	Geothermal gradient	Heat Flow
	X_1	X_2	Y_1	Y_2	Z_t	Z_o	Z_b (km)	$\frac{dT}{dz}$°C km^{-1}	q (mWm^{-2})
A	6.50	6.75	8.75	9.00	2.742	14.250	25.76	22.52	56.29
B	6.75	7.00	8.75	9.00	2.764	14.940	27.11	21.39	53.49
C	6.50	6.75	8.50	8.75	2.375	14650	26.93	21.54	53.85
D	6.75	7.00	8.50	8.75	2.674	13.620	24.57	23.61	59.02
E	7.00	7.25	8.75	9.00	2.234	14.230	26.23	22.11	55.28
F	7.25	7.50	8.75	9.00	2.282	13.260	24.24	23.93	59.82
G	7.00	7.25	8.59	8.75	4.264	14.620	24.98	23.22	58.05
H	7.25	7.50	8.59	8.75	3.985	15.790	27.60	21.01	52.54
I	6.50	6.75	8.25	8.50	2.157	16.200	30.24	19.18	47.95
J	6.75	7.00	8.25	8.50	2.256	15.450	28.64	20.25	50.63
K	6.50	6.75	8.00	8.25	1.865	14.700	27.54	21.06	52.65
L	6.75	7.00	8.09	8.25	1.987	17.123	32.36	17.98	44.95
M	7.00	7.25	8.25	8.50	2.924	14.530	26.14	22.18	59.47
N	7.25	7.50	8.25	8.50	4.093	14.150	24.21	23.96	59.89
O	7.00	7.25	8.00	8.25	2.064	14.150	26.34	22.02	55.05
P	7.25	7.50	8.00	8.25	2.903	14.710	26.52	21.87	54.68

GULU(A) **Zt = 2.742** **Zo= 14.250** **Zb= 25.76** **dt/dz = 22.52** **q=56.29**	**GULU (B)** **Zt = 2.764** **Zo= 14.940** **Zb= 27.11** **dt/dz = 21.39** **q=53.49**	**ECUJE (FCT)** **Zt = 2E.234** **Zo= 14.230** **Zb= 26.23** **dt/dz = 22.11** **q=55.28**	**KUJE (FCT)** **Zt = 2.F282** **Zo= 13.260** **Zb= 24.24** **dt/dz = 23.93** **q= 59.82**
GULU (C) **Zt = 2.375** **Zo= 14.650** **Zb= 26.93** **dt/dz = 21.54** **q=53.85**	**GULU (D)** **Zt = 2.674** **Zo= 13.620** **Zb= 24.57** **dt/dz = 23.61** **q=59.02**	**KUJE (FCT)G** **Zt = 4.264** **Zo= 14.62** **Zb= 24.98** **dt/dz = 23.22** **q=58.05**	**KUJE (FCT)H** **Zt = 3.985** **Zo= 15.790** **Zb= 27.66** **dt/dz =21.01** **q=52.54**
KONTO.KARF1(1) **Zt = 2.375** **Zo= 14.650** **Zb= 26.93** **dt/dz = 21.54** **q=53.85**	**KONTO. KARFI (J)** **Zt = 2.256** **Zo= 15.450** **Zb= 28.64** **dt/dz = 20.25** **q=50.63**	**ABAJI (M)** **Zt = 2.924** **Zo= 14.530** **Zb= 26.14** **dt/dz = 22.18** **q=59.47**	**ABAJI (N)** **Zt = 4.093** **Zo= 14.150** **Zb= 24.21** **dt/dz = 23.96** **q=59.89**
KONTO.KARFI(K) **Zt = 1.865** **Zo= 14.700** **Zb= 27.54** **dt/dz = 21.06** **q=52.65**	**KONTO.KARFI (L)** **Zt = 1.987** **Zo= 17.123** **Zb= 32.36** **dt/dz = 17.98** **q=44.95**	**ABAJI (O)** **Zt = 2.064** **Zo= 14.150** **Zb= 26.34** **dt/dz = 22.02** **q=55.05**	**ABAJI (P)** **Zt = 2903** **Zo= 14.710** **Zb= 26.52** **dt/dz = 21.87** **q=54.68**

Figure 7. Spectral blocks showing Estimated CPD, geothermal gradients and heat flow of the study area

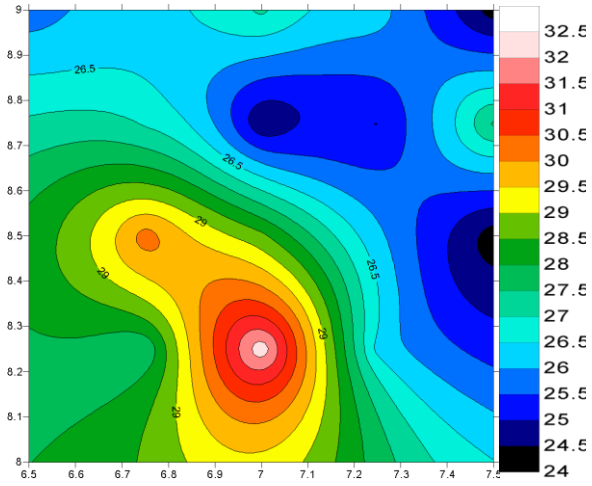

Figure 8. Spatial map of the curie point depth of the study area

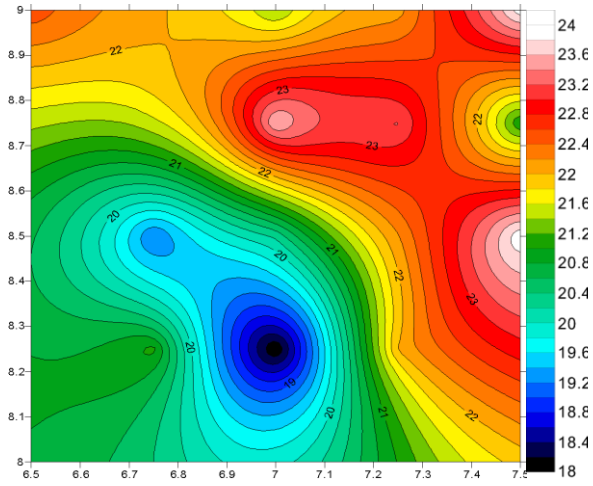

Figure 9. Spatial map of the geothermal gradient estimates of the study area

Spectral inversion of the residual field of the high resolution aeromagnetic maps over the area was carried out for the overlapping blocks using a grid size of 135 x135 km. The results of the study revealed a two layer depth model with the top layer representing the depth of magnetic sources, Z_t, while the centroid depth of magnetic sources, Z_o is represented by the bottom layer. Z_t, varies from 1.865 km to 4.264 km with an average depth of 2.723 km, while Z_o varies from 13.260 km to 17.123 km with an average depth of 14.78 km as shown in Table 1.

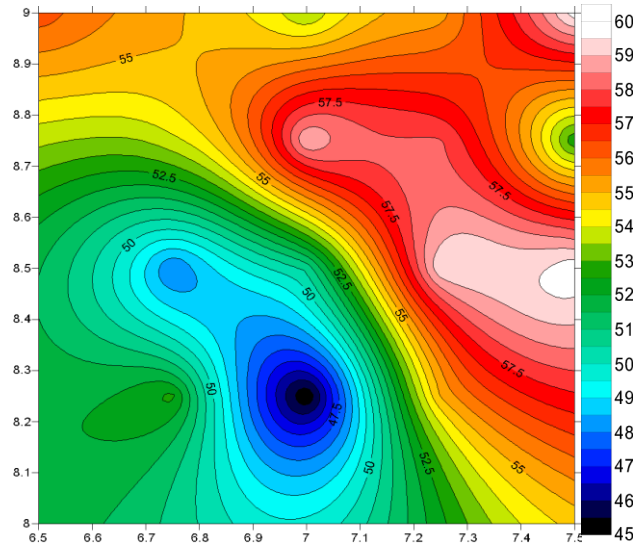

Figure 10. Spatial map of the heat flow values of the study area

Estimated values of the curie point depth, geothermal gradient, and heat flow for the various spectral blocks are shown in Table 1. Curie point depth values range from 24.21 km around the northern part of the study area to 32.26 km within the SSW section of the study area with an average depth of 26.83 km. The geothermal gradient values were estimated to be of the range of 17.98 - 23.95 ^{0}C km^{-1} with an average value of 21.62^{o}C km^{-1}. The heat flow values ranges from 44.95 mWm^{-2} to 59.89 mWm^{-2} with an average value of 54.04 mWm^{-2}.

The cross plots of CPD versus geothermal gradient and CPD versus heat flow are shown in Figures 11 &12 respectively. The coefficient of determination for the two plots revealed R^2 values between 0.9544 and 0.9999 indicating a strong correlation. The relationship between CPD and geothermal gradient, and CPD and heat flow revealed an inverse relationship. Two empirical power equations were therefore deduced from these relationships in the study area and are given as:

$$Z_b = 590.74 \left(\frac{dT}{dZ}\right)^{-1.006} \quad (11)$$

$$Z_b = 1163.5q^{-0.944} \quad (12)$$

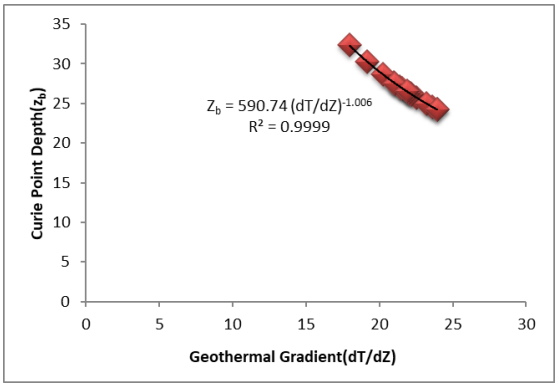

Figure 11. Cross plot of the Curie point depth versus geothermal gradient

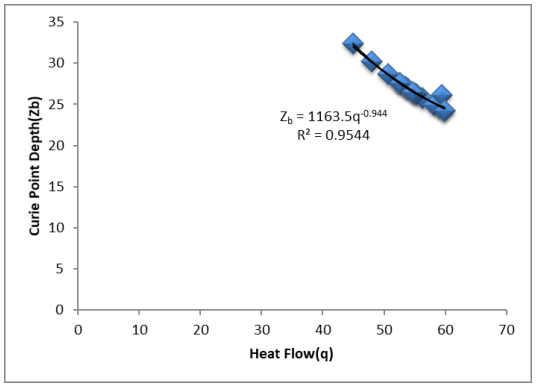

Figure 12. Cross plot of Curie point depth versus heat flow

The thermal structure of the study area is best represented by CPD based on Okubo *et al.* [36]. Okubo *et al.* [36] maintained that the pattern of the Curie point depth is useful as an index of the thermal trend because the Curie point depths estimated from the measured heat flow data of an area are very similar to those estimated from the Curie point depths analysis of the aeromagnetic data of the area. From the CPD pattern revealed in Figure 8 we can therefore infer the thermal trend of the study area. The lowest CDP values are shown at the NW, NE, and SE areas while the highest values are revealed at the SSW, and E&W parts of the study area. CPD values close to the average value are seen within the central part of the study area. The range of the CPD values (≈ 32-24 = 8km) is small and this implies that the study area falls within the same geological setting. Since the CPD values are far beyond 10km, it therefore

means that the study area is not a volcanic area or a potential geothermal reservoir. Curie point depth is greatly dependent upon geological conditions. Curie point depths are shallower than 10 km for volcanic and geothermal fields, between 15-25 km for island arcs and ridges, and deeper than 20 km in plateaus and trenches [28]. Because the average heat flow in thermally "normal" continental regions is around 60 mW/m^2, values above 80 -100 mW/m^2 indicate anomalous geothermal conditions [43]. Accordingly, areas with heat flow values greater than 60 mW/m^2 are usually recommended for further geothermal exploration. Geothermal gradients in these areas may provide potential source(s) of geothermal energy, with their Curie temperatures greater than 24^{o}C being reached at depths of less than 2 km.

The result of the geothermal gradient and heat flow regime estimated in this study is of far reaching consequences on the hydrocarbon potentials of the study area. The sedimentary thickness of the study area indicates that the potential non-marine source rocks in the area may not be deeply buried [1-3].Therefore the estimated geothermal gradient of the study area which is expected to be lower in the shallower sedimentary parts may therefore not to be enough for thermal maturation [1-2].The estimated temperature profile of the study area especially at the fringes is believed to be lower than the temperature range of the oil kitchen necessary for thermal maturation. These findings are in agreement with the results of earlier studies in the study area [1-2].

4. Summary, conclusion and recommendations

The Curie point depth, geothermal gradient, and heat flow values were estimated from the spectral inversion of the high-resolution aeromagnetic data within southern Mid-Niger Basin, Nigeria. Top depths to magnetic sources across the area are of the range of 1.865 km to 4.264 km with a mean of 2.723 km whereas the centroid depths of magnetic sources are of the range of 13.26 km to 17.12 km with a mean of 14.78 km. The range of values for the Curie point depth values varied between 24.21 km to 32.26 km with an average value of 26.83 km. The geothermal gradient values were estimated to be of the range of 17.98 - 23.95 ^{o}Ckm^{-1} with an average value of 21.62 ^{o}Ckm^{-1}. Finally, the heat flow values range from 44.95 m Wm^{-2} to 59.89 m Wm^{-2} with an average value of 54.04 m Wm^{-2}. The Curie point depth is very useful as an index of the thermal structure of an area. The range of the CPD values is small and thus indicates that the area is geologically homogenous. The CPD greater than 10km implies that the area is not a volcanic area or a potential geothermal reservoir. From the results of this study, the Mid-Niger Basin is not a potential geothermal source or prone to volcanism since the CPDs are of the range of 24.24 km and 32.26 km. Finally, the estimated geothermal gradient is not enough to lead to the thermal maturation of the the source rocks of the study area.

Acknowledgment

The authors are grateful to the Federal University of Technology, Owerri, Nigeria for sponsoring this research work. We also wish to thank the Nigerian Geological Survey Agency (NGSA) for all their support. NGSA released the high resolution aeromagnetic (HRAM) data and the geoscientific software used in this study.

References

[1] Braide SP. Petroleum geology of the Southern Bida Basin, Nigeria. Annual convention and exposition of the American Association of Petroleum Geologists, San Francisco, CA (USA), 3-6 Jun 1990, AAPG Bulletin, 1990; 74:5;

[2] Obaje NG,Moumouni A, Goki NG, and Chaanda MS. Stratigraphy, Paleogeography and Hydrocarbon Resource Potentials of the Bida Basin in North-Central Nigeria. Journal of Mining and Geology, 2011; 47(2): 97–114.

[3] Obaje NG, Bomai A, Moses SD, Ali M, Aweda A, Habu SJ, Idris-Nda A, Goro AI, and Wazir, S. Updates on the Geology and Potential Petroleum System of the Bida Basin in Central Nigeria. Petroleum Science and Engineering, 2020; 4(1):23-33.

[4] Abraham EM, Obande EG, Chukwu M, Chukwu CG, & Onwe MR. Estimating Depth to the bottom of Magnetic Sources at Wikki Warm Spring Region, Northern Nigeria, using Fractal Distribution of Sources Approach. Turkish Journal of Earth Science, 2015; 24:1–19.
[5] Nwankwo LI, Olasehinde PI, Akoshile CO. Heat flow anomalies from the spectral analysis of Airborne Magnetic data of Nupe Basin, Nigeria. Asian J. Earth Sciences, 2011; 1: 1-6.
[6] Majorowicz J, Linville A, and Osadetz KG. The relationship of hydrocarbon occurrences to geothermal gradients and time-temperature indices in Mesozoic formations of southern Alberta. Bulletin of Canadian Petroleum Geology, 1986; 34(2):226-239.
[7] Suggate RP. Relations between depth of burial, vitrinite reflectance and geothermal gradient. Journal of Petroleum Geology, 2007; 21(1): 5–32.
[8] Blackwell DD. Heat flow in the northern Basin and Range province, in The Role of Heat in the Development of Energy and Mineral Resources in the Northern Basin and Range Province, edited by Geothermal Resources Council, Spec. Rep., 1983; 13: 81–93.
[9] Bhattacharyya BK & Leu LK. Spectral analysis of gravity and magnetic anomalies due to two-dimensional structures. Geophysics, 1975; 40: 993–1013.
[10 Spector A, & Grant FS. Statistical models for interpreting aeromagnetic data. Geophysics, 1970; 35: 293–302.
[11] Byerly PE, and Stolt RH. An attempt to define the Curie point isotherm in Northern and Central Arizona. Geophysics, 1977; 42: 1394-1400.
[12] Kasidi S, Nur A. Estimation of Curie Point Depth, Heat Flow and Geothermal Gradient Inferred from Aeromagnetic Data over Jalingo and Environs North –Eastern Nigeria. International Journal Science Emerging Tech, 2013; 6: 294-301.
[13] Kasidi S, Nur A. Curie depth isotherm deduced from spectral analysis of Magnetic data over Sarti and environs of North-Eastern Nigeria. International Journal of Earth Science and Engineering, 2012; 5(1): 1284 - 1290.
[14] Stampolidis A, and Tsokas GN. Curie point depths of Macedonia and Thrace, N. Greece, Pure Appl.Geophys., 2002; 159: 2659-2671
[15] Okubo Y, Graft RJ, Hansen RO, Ogawa K, Tsu H. Curie point depths of the Island of Kyushu and surrounding areas, Japan. Geophysics, 1985; 53: 481–494.
[16] Shuey RT, Schellinger DK, Tripp AC, and Alley LB. Curie depth determination from aeromagnetic spectra. Geophys. J. the Roy. Astr. Soc., 1977; 50: 75-101.
[18] Abd-El-Nabi SH. Curie point depth beneath the Barramiya-Red Sea coast area estimated from aeromagnetic spectral analysis. Journal of Asian Earth Sciences, 2012; 43: 254–266.
[19] Sayed E, Selim I, Aboud E. Application of spectral analysis technique on ground magnetic data to calculate the Curie depth point of the eastern shore of the Gulf of Suez, Egypt. Arabian Journal of Geosciences, 2013; 7: 1749–1762.
[20] Abraham EM, Lawal KM, Ekwe AC, Alile O, Murana KA, Lawal AA. Spectral analysis of aeromagnetic data for geothermal energy investigation of Ikogosi Warm Spring–Ekiti State, southwestern Nigeria. Geothermal Energy, 2014; 2: 1–21.
[21] Obande GE, Lawal KM, Ahmed LA. Spectral analysis of aeromagnetic data for the geothermal investigation of WikkiWarm Spring, North-east Nigeria. Geothermics, 2014; 50: 85–90.
[22] Saleh S, Salk M, Pamukcu O. Estimating Curie point depth and heat flow map for Northern Red Sea rift of Egypt and its surroundings, from aeromagnetic data. Pure and Applied Geophysics, 2013; 170: 863–885.
[23] Hsieh HH, Chen CH, Lin PY, Yen HY. Curie Point Depth from Spectral Analysis of Magnetic data in Taiwan. Journal of Asian Earth Sciences, 2014; 90: 26 – 33.
[24] Bhattacharyya BK. Continuous spectrum of the total Magnetic field Anomaly due to Rectangular Prismatic Body. Geophysics, 1966; 31(1): 97 – 121.
[25] Okubo Y, Tsu H, Ogawa K. Estimation of Curie Point Temperature and Geothermal Structure of Island Areas of Japan, Tectonophysics, 1989; 159: 279 – 290.
[26] Bansa, AR, Anand SP, Rajaram M, Rao VK, Dimri VP. Depth to the bottom of magnetic sources (DBMS) from aeromagnetic data of Central India using a modified centroid method for fractal distribution of sources. Tectonophysics, 2013; 603: 155–161.
[27] Tanaka A, Okubo Y, Matsubayashi O. Curie point depth based on spectrum Analysis of the magnetic anomaly data in East and Southeast Asia. Tectonophysics, 1999; 306: 461–470.
[28] Ladipo KO. Paleogrogaphy Sedimentation and Tectonics of the upper Cretacemes Anambra Basin, South-eastern Nigeria. Journal of African Earth Sciences, 1988; 7: 865 – 871.
[29] Obaje N, Wehner H, Scheeder G, Abubakar K, Jauro A. Hydrocarbon prospectivity of Nigeria's inland basins.From the viewpoint of organs geochemistry and organic petrology. AAPG Bulletin, 2004; 88(3): 325 – 353.

[30] Obaje N, Musa M, Odoma A, Hamza H. The Bida Basin in North-central Nigeria: sedimentology and petroleum geology. J. Petroleum and Gas Exploration Research,2011; 1(1): 001–013.
[31] Obaje HG. Geology and Mineral Resources of Nigeria. Lecture Notes in Earth Sciences; 2009; 120: 221p. DOI.10.1007/978-3-540-92685-6.
[32] Ojo S B. Middle Niger Basin revisited: Magnetic Constraints on Gravity Interpretation Abstract, 20th Conference of the Nigeria Mining and Geosciences Society 1984, Nsukka, 52 – 53.
[33] Udensi EE, Ozazwa IB. Spectral determination of depths to magnetic rocks under the Nupe Basin, Nigeria. Nigerian Associations of Petroleum explorationists (NAPE), Bull, 2004; 17: 22–27.
[34] Blakely RJ. Potential Theory in Gravity and Magnetic Applications, Cambridge Univ. Press 1995, Cambridge, U. K.
[35] Hsieh H-H, Chen Ch-H, Lin P-Y, and Yen H-Y. Curie point depth from spectral analysis of magnetic data in Taiwan. Journal of Asian Earth Science, 2014; 90: 26- 33
[36] Okubo Y, Tsu H, Ogawa K. Estimation of Curie point temperature and geothermal structure of island arcs of Japan.Tectonophysics, 1989; 159: 279–290.
[37] Okubo Y, Matsushima J, Correia A. Magnetic spectral analysis in Portugal and its adjacent seas. Phys Chem Earth, 2003; 28: 511–519.
[38] Salem A, Green C, Ravat D, Singh KH, East P, Fairhead JD, Mogren S, & Biegert E. Depth to Curie temperature across the central Red Sea from magnetic data using the de-fractal method. Tectonophysics, 2014; 624(62): 75–86.
[39] Tselentis A. An attempt to define Curie point depths in Greece from aeromagnetic and heat flow data. Pure and Applied Geophysics, 1991; 136(1): 87-101.
[40] Okubo Y, Matsunaga T Curie point depth in northeast Japan and its correlation with regional thermal structure andseismicity. J Geophys Res., 1994; 99: 22363–22371.
[41] Nwankwo LI, Olasehinde PI, & Akoshile CO. An attempt to estimate the Curie Point Isotherm depth in the Nupe Basin, west Central Nigeria. Global Journal of Pure and Applied Sciences, 2009; 15(3): 427 – 433.
[42] Stacey FD. Physics of the Earth. 2nd ed. John Wiley & Sons 1977, New York, USA.
[43] Jessop AM, Hobart MA, and Sclater JG. The world heat flow data collection 1975. Geothermal Services of Canada. Geotherm Ser., 1976; 50: 55-77.

To whom correspondence should be addressed: professor A. I. Opara, Department of Geology, Federal University of Technology, Owerri, Nigeria, E-mail: oparazanda2001@yahoo.com